Neurobiology of Aging xxx (2013) 1–6

Contents lists available at SciVerse ScienceDirect

Neurobiology of Aging

journal homepage: www.elsevier.com/locate/neuaging

Amyloid β peptides modify the expression of antioxidant repair enzymes and a potassium channel in the septohippocampal system

Jorge Durán-González [a], Edna D. Michi [a], Brisa Elorza [a], Miriam G. Perez-Córdova [a], Luis F. Pacheco-Otalora [a], Ahmed Touhami [b], Pamela Paulson [a], George Perry [c], Ian V. Murray [d], Luis V. Colom [a,e,*]

[a] Center for Biomedical Studies, The University of Texas at Brownsville, Brownsville, TX, USA
[b] Physics and Astronomy Department, The University of Texas at Brownsville, Brownsville, TX, USA
[c] Biology Department, The University of Texas at San Antonio, San Antonio TX, USA
[d] Department of Neuroscience and Experimental Therapeutics, University of Texas A&M, Bryan, TX, USA
[e] Department of Biomedicine, The University of Texas at Brownsville, Brownsville, TX, USA

ARTICLE INFO

Article history:
Received 30 July 2012
Received in revised form 20 December 2012
Accepted 9 February 2013

Keywords:
Alzheimer
Amyloid β
Potassium currents
Gene expression profile

ABSTRACT

Alzheimer's disease (AD) is a progressive, neurodegenerative brain disorder characterized by extracellular accumulations of amyloid β (Aβ) peptides, intracellular accumulation of abnormal proteins, and early loss of basal forebrain neurons. Recent studies have indicated that the conformation of Aβ is crucial for neuronal toxicity, with intermediate misfolded forms such as oligomers being more toxic than the final fibrillar forms. Our previous work shows that Aβ blocks the potassium (K^+) currents I_M and I_A in septal neurons, increasing firing rates, diminishing rhythmicity and firing coherence. Evidence also suggests that oxidative stress (OS) plays a role in AD pathogenesis. Thus we wished to determine the effect of oligomeric and fibrillar forms of $A\beta_{1-42}$ on septohippocampal damage, oxidative damage, and dysfunction in AD. Oligomeric and fibrillar forms of $A\beta_{1-42}$ were injected into the CA1 region of the hippocampus in live rats. The rats were sacrificed 24 hours and 1 month after Aβ or sham injection to additionally evaluate the temporal effects. The expression levels of the K^+ voltage-gated channel, KQT-like subfamily, member 2 ($KCNQ_2$) and the OS-related genes superoxide dismutase 1, 8-oxoguanine DNA glycosylase, and monamine oxidase A, were analyzed in the hippocampus, medial, and lateral septum. Our results show that both forms of Aβ exhibit time-dependent differential modulation of OS and K^+ channel genes in the analyzed regions. Importantly, we demonstrate that Aβ injected into the hippocampus triggered changes in gene expression in anatomical regions distant from the injection site. Thus the Aβ effect was transmitted to anatomically separate sites, because of the functional coupling of the brain structures.

1. Introduction

Alzheimer's disease (AD) is a progressive, neurodegenerative disorder that causes memory loss, dementia, and death. The more common sporadic form of AD is correlated with aging, and the increase of life expectancy is transforming AD into a major health problem in the developed and developing world. Although the mechanisms that lead to brain dysfunction and neurodegeneration in AD are not clearly understood, extracellular accumulation of amyloid beta peptides (Aβ) is a defining feature of this pathology, leading to the idea that amyloid accumulation plays an important role in the development of the disease.

One of the main pathological features of AD is the pathological misfolding of Aβ to adopt a β-sheet conformation (Di Carlo et al., 2012). This occurs via a nucleated polymerization mechanism; this involves the formation of soluble, oligomeric intermediate pathogenic species, and terminating with the formation of fibrillar Aβ, which are now thought to be nonpathogenic (Fändrich, 2012).

Oxidative damage is observed in the brain of AD patients (Butterfield et al., 2001) and oxidative stress (OS) leads to an increased Aβ production that, in turn, exacerbates OS (Irie et al., 2007; Murray et al., 2007; Tong et al., 2005). Thus, OS and increased Aβ might create a deleterious cycle that concludes with membrane damage, cytoskeleton alterations, and cell death (Perry et al., 2000). Some of the proposed mechanisms behind AD and OS include the Aβ interaction with redox active metal ions, which

* Corresponding author at: Center for Biomedical Studies, The University of Texas at Brownsville, 80 Fort Brown, Brownsville, TX 78520, USA. Tel.: +1 956 882 5048; fax: +1 956 882 6810.
E-mail address: luis.colom@utb.edu (L.V. Colom).

0197-4580/$ – see front matter © 2013 Elsevier Inc. All rights reserved.
http://dx.doi.org/10.1016/j.neurobiolaging.2013.02.005

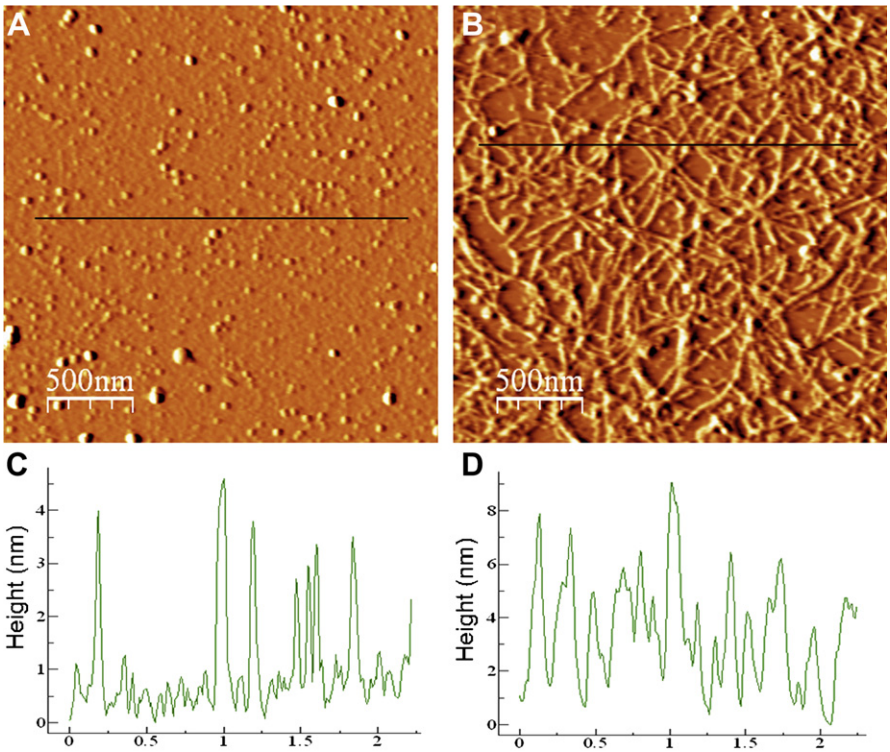

Fig. 1. (A) Deflection atomic force microscopy (AFM) image of the oligomeric amyloid beta (Aβ) showing single and aggregate proteins. (B) Deflection AFM image of the fibrillar Aβ indicating the coexistence of fibrils and single proteins (fibrils have various lengths). (C) AFM cross-section along the line shown in (A) (black line). The Aβ oligomers are approximately 4 nm in size. (D) AFM cross-section along the line shown in (B). The width of the single Aβ fibrils is approximately 8 nm.

are a significant source of OS, inducing neurotoxicity via cell-free hydrogen peroxide generation (Huang et al., 1999) in a protective pathway that includes the activity of the enzyme superoxide dismutase (SOD1) as an intermediate step (Marlatt et al., 2004). Another major modification is the oxidative damage of DNA. Mutations in mitochondrial DNA cause a respiratory chain dysfunction, which can increase cellular OS. It is established that mitochondrial mutations accumulate during brain aging and neurodegenerative diseases (Santos et al., 2010). Although several oxidized bases can result from attack on DNA by OS, the predominant marker is 8-hydroxy-2′-deoxyguanosine (8-OHdG), that induces a G:C → A:T transversion (Shibutani et al., 1991), reverted mainly by the antioxidant enzyme 8-oxoguanine DNA glycosylase (OGG1) (Tchou et al., 1991). New evidence suggests impaired function of enzymes related to recycling neurotransmitters like monoamine oxidase (MAO) are indirect generators of cytotoxic free-radicals during aging and in neurodegenerative diseases (Richards et al., 1998). Because of the relevant role of these enzymes in oxidative damage and protection from this type of insult, we postulate that the presence of increased concentrations of Aβ forms could lead to a modified response in their gene expression and that this change might contribute to the progression of this disorder within the brain.

Our previous studies have shown that administration of fibrillar Aβ into the hippocampus leads to the formation of localized Thioflavin S-positive amyloid β lesions in the hippocampus and a reduction of medial septum neuronal numbers, suggesting a complex damage response network (Colom et al., 2011). Furthermore, Aβ excess produces brain dysfunction and degeneration via modification of potassium (K^+) currents (e.g., I_M, I_A, and I_K) (Colom et al., 1998; Leão et al., 2012), that will result in: (1) loss of rhythmic states that promote synaptic plasticity and memory formation (Colom et al., 2010; Leão et al., 2012); (2) hyperexcitability, including epilepsy, as found in AD patients and animal models (Noebels, 2011); and (3) cell death mechanisms (Colom et al., 1998). The neurotransmitter-modulated I_M current is carried in the brain mainly by the $KCNQ_{2/3}$ subunits and is particularly affected by oligomeric Aβ in glutamatergic septal neurons (Leão et al., 2012) and, thus, might play a role in the memory loss observed in AD patients.

In the present study, we analyze the expression of the OS-related genes SOD1, OGG1, and MAOA, and the K^+ channel subunit $KCNQ_2$ ($K_v7.2$) in the hippocampus, medial, and lateral septum after hippocampal CA1 exposure to oligomeric and fibrillar forms of Aβ.

2. Methods

2.1. Animals

A total of 24 adult Sprague Dawley rats (9 weeks old, and weight 250–300 g; Harlan) were housed and maintained on a 12-hour light/dark cycle and provided food and water ad libitum. All animal protocols used in this study were in compliance with the National Institutes of Health Guide for the Care and Use of Laboratory Animals and approved by the Institutional Animal Care and Use Committee of the University of Texas Brownsville and Texas Southmost College (UTB/TSC). All surgical procedures were performed with a ketamine-based anesthetic (ketamine: 43.2 mg/mL, xylazine: 8.6 mg/mL, and acepromazine: 1.35 mg/mL in saline; 1 mL/kg). Groups of rats were sacrificed for gene analysis at 24 hours and 1 month after Aβ injection or sham treatment.

2.2. Aβ preparation

2.2.1. Oligomers

$Aβ_{1–42}$ and $Aβ_{42–1}$ (.5 mg each) (California Peptide) were dissolved in 22 μL of anhydrous dimethyl sulfoxide (DMSO) to yield

a 5 mM solution, then diluted to a concentration of 100 μM by adding 490 μL of phosphate buffered saline (PBS) pH 7.4 and 10 μL of DMSO solution. Amyloid β oligomers were then generated by incubation for 17 hours at 4 °C (De Felice et al., 2008).

2.2.2. Fibrils

$A\beta_{1-42}$ and $A\beta_{42-1}$ (.5 mg each) (California Peptide) were dissolved in 22 μL of anhydrous dimethyl sulfoxide (DMSO) to yield a 5 mM solution, 10 μL was further diluted to 100 μM solution by adding 490 μL of hydrochloric acid (HCL) (10 mM). Fibrillar amyloid was formed by incubation for 87 hours at 37 °C (De Felice et al., 2008).

2.3. Atomic force microscopy

Atomic force microscopy (AFM) was used to confirm the oligomeric and fibrillary forms of the Aβ preparations. A 1-μL portion from each Aβ solution (previous paragraph) was diluted 10 times using PBS 7.4 pH. Then approximately 50-μL drops from each solution were incubated at room temperature for 30 minutes with 2 freshly-cleaved mica surfaces. The samples were rinsed 5 times with deionized water to remove the nonadsorbed proteins. Finally, the samples were air-dried for 30 minutes and imaged in air. AFM measurements were performed in contact mode at room temperature using a Multimode AFM with a Nanoscope IV Controller (Digital Instruments, Veeco, Santa Barbara, CA, USA) and V-shaped Si_3N_4 cantilevers with oxide-sharpened tips (Olympus; spring constant of 0.15 N/m). As can be seen in Fig. 1A, the oligomeric Aβ peptide homogeneously covers the mica surface and appears as single beads or small aggregates. The AFM cross-section (Fig. 1C) shows that the size of these single beads is approximately 4 nm which is similar to the average size of a single Aβ protein. The fibrillar Aβ peptide is a mixture of short fibrils (with various lengths) and a single protein (Fig. 1B). As shown in Fig. 1D the width of the fibrils is approximately 8 nm which is twice the size of a single Aβ peptide.

2.4. Aβ injections

Rats were anesthetized using a combination of anesthetics (0.3 mL/kg, containing ketamine [42.8 mg/mL], xylazine [8.6 mg/mL], and acepromazine [1.4 mg/mL]), and unilateral microinjections of $A\beta_{1-42}$ (oligomeric and fibrillar forms as separated groups) (10 μg in 5 μL of sterile PBS) were administered into the CA1 region of the hippocampus using stereotaxic coordinates derived from the Paxinos and Watson atlas (3.4–3.6 mm posterior from bregma, 2 mm lateral, and 2.3–2.5 mm vertical) (Paxinos and Watson, 1998). All microinjections were administered using a 10-μL Hamilton syringe which was slowly lowered into the CA1 hippocampal region. The needle was left in place for approximately 10 minutes before the injection of peptide. Thereafter, $A\beta_{1-42}$ was injected at a rate of 1 μL per minute. The needle was left in place for an additional 10 minutes after the injection of Aβ to prevent transport of the peptide up the needle tract. Control rats received a unilateral hippocampus microinjection of identical volume of the reverse oligomeric and fibrillar peptides $A\beta_{42-1}$, following the same protocol.

2.5. Medial septum/diagonal band, lateral septum, and hippocampal extraction of tissue

To evaluate the influence of Aβ conformation and time of exposure to the peptides on gene expression, we analyzed the previously described specific genes. The injected animals were divided in 2 groups, 24 hours and 1 month after Aβ injection. The first group (24 hours) was evaluated for short-term effects of Aβ and the second group (1 month) was evaluated for chronic exposure to Aβ and sacrificed 30 days after the injection.

Rats were deeply anesthetized using a combination of anesthetics (0.7 mL/kg, containing ketamine [42.8 mg/mL], xylazine [8.6 mg/mL], and acepromazine [1.4 mg/mL]) and rapidly decapitated. The brain was then removed and immersed in ice-cold, diethylpyrocarbonate (DEPC)-treated PBS aerated with 95% O_2 and 5% CO_2 to equilibrate the pH at 7.3–7.4. The brain was mounted on a plastic tray with cyanoacrylate glue. Coronal slices (300 μm thick) containing the medial septum/diagonal band (MS) were prepared using a vibratome (OTS-4000; EMS, Hatfield, PA, USA). The MS and lateral septum (LS) structures of the basal forebrain were carefully dissected using 25-gauge needles. MS and LS slices were transferred into RNAlater solution (Applied Biosystems) for later processing.

After slicing the medial septum, the remaining brain tissue was unglued from the tray and placed into a petri dish (filled with DEPC-treated PBS and aerated with 95% O_2 and 5% CO_2). The hippocampus was removed parasagittally and immediately transferred into a microtube filled with PBS-DEPC RNAlater solution.

2.6. RNA isolation, cDNA library, and real-time quantitative polymerase chain reaction analysis

Total RNA was isolated from the dissected hippocampus, lateral, and medial septum. In brief, tissue was collected, weighed, homogenized, and processed for total RNA isolation at 4 °C using RNAqueous-4PCR Kit (Applied Biosystems) following the manufacturer's instructions. The concentration and purity of total RNA for each sample was determined with a Nanodrop ND-1000 Spectrophotometer (Thermo Scientific, Wilmington, DE, USA) by calculating the ratio of optical density at wavelengths of 260 nm and 280 nm. Trace amount of genomic DNA contamination were minimized by digesting genomic DNA using DNA-free DNase Treatment (Applied Biosystems) following the manufacturer's protocols. Reverse transcription (RT) was performed with an iCycler Thermal Cycler polymerase chain reaction (PCR) System (Bio-Rad Laboratories, Hercules, CA, USA), using the High Capacity cDNA Reverse Transcription Kit (Applied Biosystems) for synthesis of a single-stranded cDNA library. The cDNA synthesis was carried out according to the manufacturer's protocol using random primers for 1 μg of starting RNA. Each RT reaction contained 1 μg of extracted total RNA template and RT reagents. The 20-μL reactions were incubated for 10 minutes at 25 °C, 120 minutes at 37 °C, 5 seconds at 85 °C, and then held at 4 °C. The resulting cDNA template was subjected to real-time quantitative PCR using Taqman-based ABI gene expression assays, TaqMan Fast Universal PCR Master Mix (ABI), and the StepOne real-time thermocycler engine (ABI). Gene expression analysis was performed using the following assays: Rn00566938_m1 for target gene SOD1 (RefSeq: NM_017050.1), Rn00578409_m1 for target gene OGG1 (RefSeq: NM_030870.1), Rn00591249_m1 for target gene KCNQ2 (Ref Seq NM_133322.1), Rn01430950_m1 for target gene MAOA (RefSeq: NM_033653.1), and the bioassay Rn99999916_s1 for the normalization gene glyceraldehyde-3-phosphate dehydrogenase (GAPDH; RefSeq: NM_017008.3). Each sample was run in triplicate and a non-template control to test for contamination of assay reagents was also included in the plate. After a 94 °C denaturation for 10 minutes, the reactions were cycled 40 times with a 94 °C denaturation for 15 seconds, and 60 °C annealing for 1 minute. Three types of controls aimed at detecting genomic DNA contamination in the RNA sample or during the RT or quantitative PCR reactions were always included: an RT mixture without reverse transcriptase, an RT mixture including the enzyme but no RNA, and a negative control (reaction mixture without cDNA template). The data were

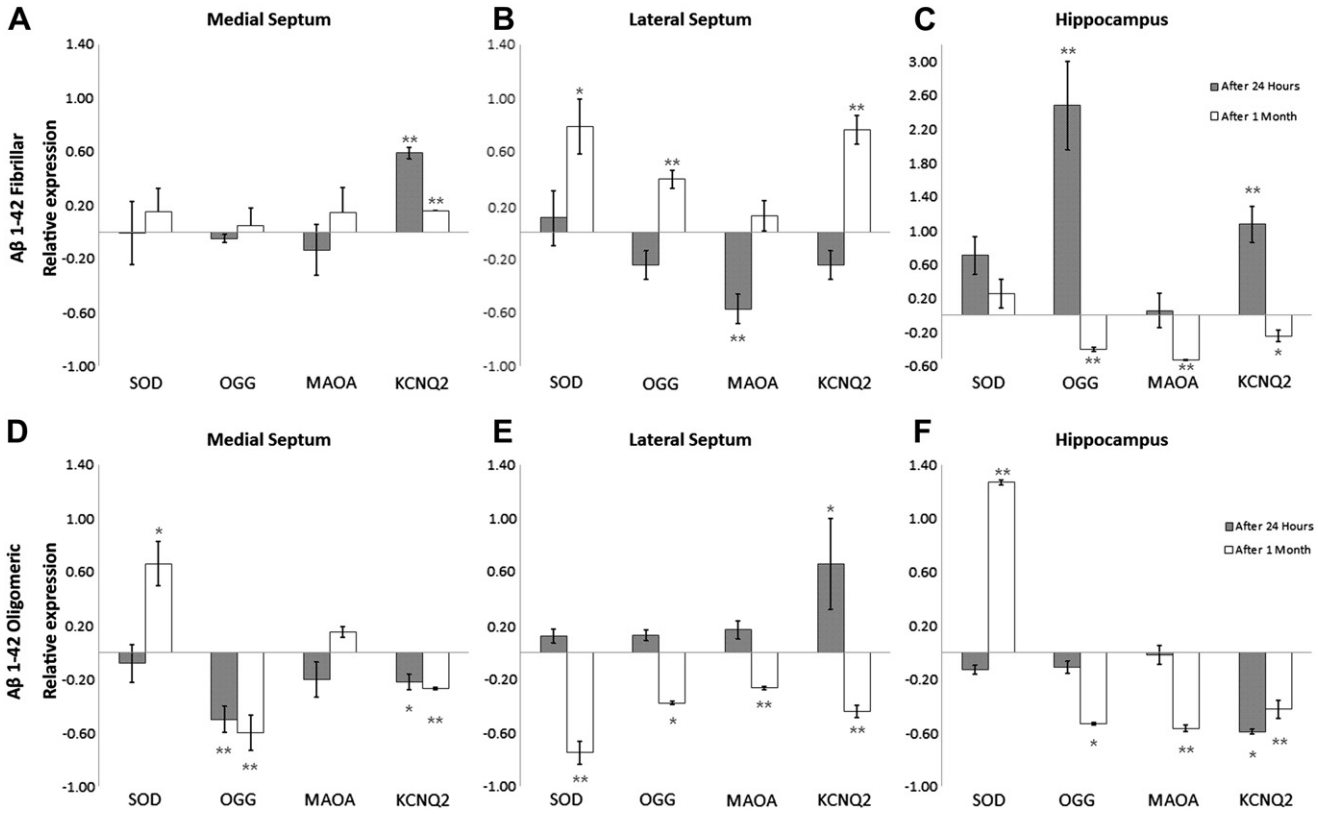

Fig. 2. Relative expression of SOD, OGG, MAOA, and $KCNQ_2$ genes with altered messenger RNA (mRNA) levels in the (A, B, and C) fibrillar and (D, E, and F) oligomeric analyzed groups. Expression levels of the genes were analyzed by quantitative reverse transcription polymerase chain reaction and normalized over GAPDH. $^{*}p < 0.05$, $^{**}p < 0.001$ (when compared with respective reverse peptide controls). Error bars indicate standard error. Abbreviations: Aβ, amyloid beta; GAPDH, glyceraldehyde-3-phosphate dehydrogenase; $KCNQ_2$, potassium voltage-gated channel, KQT-like subfamily, member 2; MAOA, monoamine oxidase A; SOD, superoxide dismutase.

collected and analyzed using OneStep Software version 2.2.2 (ABI). Relative quantification was performed using the comparative threshold (CT) method after determining the CT values for reference (GAPDH) and target (SOD1, OGG1, KCNQ2, and MAOA) genes in each sample set according to the ΔΔCT method (Pfaffl, 2006) as described by the manufacturer (Applied Biosystems; User Bulletin 2). Changes in messenger RNA (mRNA) expression level were calculated after normalization to GAPDH. As a calibrator sample, we used cDNA from an arbitrarily selected control rat. Values of fold changes in the control sample versus the Aβ-injected samples represent averages from triplicate measurements. Changes in gene expression were reported as percent changes relative to controls. Data were analyzed by 1-way analysis of variance with a significance p value set at <0.05.

3. Results

3.1. MS

Overall, in the 24-hour group, the analyzed OS genes were downregulated in the medial septum after injection of oligomeric and fibrillar Aβ. The largest change occurred in OGG1 expression (-0.50 ± 0.09; $p < 0.001$) in the rats injected with the oligomeric form of Aβ (Fig. 2D). Though the expression of the KCNQ2 gene was reduced in the group injected with oligomeric Aβ (-0.22 ± 0.06; $p < 0.05$), this gene was significantly overexpressed (0.58 ± 0.04; $p < 0.001$) in the group injected with the fibrillar form (Fig. 2A).

The chronic effects (after 1 month) of oligomeric Aβ differed from that of rats exposed to oligomeric Aβ for 24 hours. The downregulation of the OGG1 (-0.60 ± 0.13; $p < 0.001$) and $KCNQ_2$ (-0.27 ± 0.01; $p < 0.001$) genes were maintained, but the level of SOD1 (0.66 ± 0.16; $p < 0.001$) was significantly increased, and MAOA (not significant) showed a lesser increase (Fig. 2D).

3.2. LS

Gene expressions in the lateral septum for the 24-hours injected group was more diverse than the medial septum with opposite effects being observed for the 2 forms of Aβ. Though the same genes were downregulated as in the medial septum, the MAOA gene was more vulnerable and exhibited greater downregulation (-0.58 ± 0.11; $p < 0.001$) than fibrillar Aβ (Fig. 2B).

In contrast to the effects of the fibrillar form, the oligomeric Aβ resulted in increased expression of all the studied genes in the lateral septum, with KCNQ2 (0.66 ± 0.3; $p = 0.03$) showing the higher values (Fig. 2E). Though not significant, both forms of Aβ resulted in an upregulation of the SOD1 gene maintained in the lateral septum.

After 30 days after Aβ injection, the response was reversed for both forms of Aβ. There was an overall downregulation among all investigated genes in animals injected with the oligomeric form: SOD1 (-0.75 ± 0.08; $p < 0.001$), OGG1 (-0.38 ± 0.01; $p = 0.01$), MAOA (-0.27 ± 0.01; $p < 0.001$), and $KCNQ_2$ (-0.45 ± 0.04; $p = 0.001$) (Fig. 2E); and with fibrillar Aβ there was overexpression in the analyzed genes SOD1 (0.79 ± 0.2; $p = 0.003$), OGG1 (0.39 ± 0.07; $p < 0.001$), MAOA (0.12 ± 0.01; $p =$ not significant), and $KCNQ_2$ (0.76 ± 0.04; $p < 0.001$) (Fig. 2B).

3.3. Hippocampus

After 24 hours after intrahippocampal injection with fibrillar Aβ, all the analyzed genes were overexpressed (Fig. 2C). However, the

effect of injection of oligomeric Aβ in the hippocampus was totally opposite: KCNQ2 showed a significant reduction in expression (-0.59 ± 0.01; $p < 0.001$). The most remarkable results were in the chronic group (1 month) because both Aβ forms showed the same expression profile for all analyzed genes (Fig. 2C and F).

4. Discussion

We selected the rat as a model to investigate the time-dependent effect of Aβ conformation (oligomeric of fibrillar) on a group of genes relevant in AD pathophysiology: specifically, the $KCNQ_2$ ion channel and OS markers. We selected young adult rats for our experimentation based on the following rationale. Though AD is an aging-related brain disorder, Aβ deposition and functional alterations start many years before AD diagnosis (Holtzman, 2008; Verghese et al., 2011). Even more, in commercially recognized rat models, Alzheimer pathology can be induced in young rats (Lecanu et al., 2006). Thus, it is important to investigate Aβ effects in young, adult, and aged animals to determine the molecular changes that might trigger the initiation of AD dysfunction and pathology.

We demonstrate that intrahippocampal administration of Aβ modified the gene expression in several brain areas: hippocampus and medial and lateral septum. Because the septohippocampal system plays a central role in memory processes affected in AD and the septal region has been implicated in mood disorders frequently observed in AD (Colom et al., 2006), the observed changes in these brain lesions might be particularly relevant to the pathogenesis of this disorder.

Intrahippocampal administration of Aβ produced changes in 2 basal forebrain structures with different neuronal populations and connectivity. We propose that the septal changes can be explained by the following mechanisms: (1) Aβ could directly affect presynaptic terminals of septohippocampal neurons, leading to alterations in other neuronal compartments; (2) Aβ could alter the function and damage hippocampal neurons, leading to gene expression alteration in the synaptically connected brain structures; or (3) a combination of both mechanisms.

The medial septal brain region is composed of cholinergic, glutamatergic, and GABAergic neurons, with neurons in each of these neuronal populations projecting to the hippocampus. As feedback, the medial septum receives a small projection from hippocampal GABAergic neurons (Colom et al., 2006). The lateral septum is mostly composed of GABAergic neurons, and receives glutamatergic projection from the hippocampus, but does not project to the hippocampus. Because the hippocampus does not receive input from lateral septal axons, a retrograde feedback mechanism cannot explain the lateral septal alterations produced by hippocampal perturbations, such as Aβ accumulation.

We propose the following "activity-dependent" model that is consistent with our previous work and provides an explanation of our current results. Initially, administration of oligomeric Aβ blocks I_M and I_A K^+ conduction in septal neurons (Leão et al., 2012). In the hippocampus, the expression of the $KCNQ_2$ is probably reduced by the Aβ-induced damage. We propose that Aβ, through the K^+ channel block, rapidly increases the firing rates of hippocampal principal and GABAergic interneurons, impairing rhythmicity and synchronic activities. As a result of this alteration, hippocampal outputs are also modified. The hippocampal–medial septal output is GABAergic, and thus, an increase in its activity will lead to medial septal inhibition with consequent reduction of OS gene expression as observed in the acute oligomeric Aβ-treated group. To compensate for the reduced neuronal activity in the medial septum, the expression of the $KCNQ_2$ gene is lowered. In contrast, the hippocampal–lateral septal output is glutamatergic and its activation will intensify lateral septal network activity with consequent increases of OS gene expression. Thus in the lateral septum, the expression of the $KCNQ_2$ gene is augmented to compensate for the intensification of neuronal activity.

During the following weeks, with chronic oligomeric Aβ treatment, this reduced expression of $KCNQ_2$ was maintained and extended to the lateral septum, probably indicating a failed compensatory response to restore to the natural and pre-Aβ injection status. These results illustrate that Aβ can lead to a reduced expression of the $KCNQ_2$ gene in functionally related structures and prove that K^+ channel genes are susceptible to oligomeric Aβ influence. Finally, fibrillary Aβ is less effective in modulating K^+ channels (Leão et al., 2012) and its neurotoxicity is probably related to alternative mechanisms (e.g., delayed I_K enhancement; Colom et al., 1998), producing different patterns of OS and K^+ channel gene expression.

Our work also demonstrates changes in OS markers. We show that: (1) the analyzed OS-related genes modify their expression profile under the influence of Aβ; (2) those changes appear in a short period of time; and (3) changes in function and neuronal damage might involve multiple OS pathways and that OS changes might be related to functional changes. Our "activity-dependent" model predicts early changes after oligomeric Aβ accumulation. Later changes need to incorporate compensatory mechanisms that are not yet fully understood.

For example, the expression of the antioxidant gene (SOD1) is affected by the administration of oligomeric Aβ. An early decreased expression followed by a significant overexpression was observed in the medial septum and the hippocampus. Late increases were not observed in the lateral septum. Because SOD1 has antioxidant roles, lower levels of SOD1 in the lateral septum might increase its vulnerability to gradual accumulation of reactive oxygen species, contributing to Aβ-induced damage. These results can be correlated with the work of Kent and collaborators (Kent et al., 1999) who demonstrated that lower expression of the SOD1 gene is a common feature in the brain of aging rodents, but a compensatory overexpression could also result in an increased toxicity because of the excessive conversion of superoxide to O_2 and H_2O_2 (the main function of SOD1). Thus, the alterations in the expression of this gene play an important role in the early stages and progression of AD.

Also, OS induction of modifications on DNA sequences might critically contribute to the brain damage. Any maintained DNA damage becomes irreparable (Freitas and de Magalhães, 2011) To avoid this negative outcome, DNA oxidation is repaired by OGG1 in nuclear and mitochondrial fractions (Wang et al., 2011). With aging, the levels of OGG1 decrease in the mitochondria of different tissues, suggesting a reduced repair capability (Stevnsner et al., 2002). Our work shows that oligomeric Aβ significantly decreases the expression profile of the DNA repair gene OGG1 and suggests that lessened repair mechanisms might contribute to the Aβ-induced damage. Although the present study did not investigate the occurrence of new mutations in nuclear or mitochondrial fractions, our results suggest that any change in DNA by the most common mutagenic element, 8-OHdG, can lead to permanent DNA modifications because of the lower expression levels of the OGG gene. These lower expression levels might produce an impaired damage response with devastating consequences in AD, particularly in mitochondrial RNA (Lin et al., 2011; Wang et al., 2011). The lack of DNA repair capability might contribute to neurodegeneration and cell dysfunction. Because it has been reported that OGG activity shows an inverse correlation with levels of 8-OHdG in mild cognitive impairment and AD, DNA changes might play an important role in the development of the disorder before the full expression of AD symptomatology (Shao et al., 2008).

It has been proposed that neurodegeneration with subsequent reduction of neuronal populations can trigger diverse compensatory responses from the remaining neurons in the brain, including an increased expression of the mRNA levels of the MAOA gene, as

observed in postmortem neurons of AD patients (Emilsson et al., 2002). Because MAO is an indirect generator of cytotoxic free-radicals, this overexpression can lead to more OS, as observed in aging and AD (Hermida-Ameijeiras et al., 2004; Richards et al., 1998). In the present work, the MAOA gene expression was most robustly reduced in the lateral septum after chronic exposure (1 month) to Aβ. A decreased expression of MAOA in the hippocampus under the influence of both Aβ forms was also observed, suggesting that increased expression profiles might not be a part of early stages of AD.

Independent of the mechanisms underlying the proposed changes, we provide evidence that limited deposition of Aβ resulted in modified gene expression in several functionally-related brain structures. We demonstrated that gene expression changes do not require Aβ contact with dendrosomatic neuronal compartments and that the presence of: (1) presynaptic terminals in close proximity with Aβ deposits; or (2) simply Aβ-triggered functional changes, might be sufficient to alter gene expression in functionally related brain structures. Thus, Aβ accumulation might lead to neuronal dysfunction and damage that could not be fixed because of the reduced of expression of repairing genes.

Disclosure statement

The authors report no conflicts of interest.

All animal protocols used in this study were in compliance with the National Institutes of Health Guide for the Care and Use of Laboratory Animals and approved by the Institutional Animal Care and Use Committee of the University of Texas Brownsville and Texas Southmost College (UTB/TSC).

Acknowledgements

This study was supported by National Institutes of Health grants 5S06GM0688550 (Luis V. Colom) and G12-MD007591 (George Perry).

References

Butterfield, D.A., Drake, J., Pocernich, C., Castegna, A., 2001. Evidence of oxidative damage in Alzheimer's disease brain: central role for amyloid beta-peptide. Trends Mol. Med. 7, 548–554.

Colom, L.V., Castañeda, M.T., Bañuelos, C., Puras, G., García-Hernández, A., Hernandez, S., Mounsey, S., Benavidez, J., Lehker, C., 2010. Medial septal beta-amyloid 1-40 injections alter septo-hippocampal anatomy and function. Neurobiol. Aging 31, 46–57.

Colom, L.V., Castaneda, M.T., Hernandez, S., Perry, G., Jaime, S., Touhami, A., 2011. Intrahippocampal amyloid-β (1–40) injections injure medial septal neurons in rats. Curr. Alzheimer Res. 8, 832–840.

Colom, L.V., Diaz, M.E., Beers, D.R., Neely, A., Xie, W.J., Appel, S.H., 1998. Role of potassium channels in amyloid-induced cell death. J. Neurochem. 70, 1925–1934.

Colom, L.V., García-Hernández, A., Castañeda, M.T., Perez-Cordova, M.G., Garrido-Sanabria, E.R., 2006. Septo-hippocampal networks in chronically epileptic rats: potential antiepileptic effects of theta rhythm generation. J. Neurophysiol. 95, 3645–3653.

De Felice, F.G., Wu, D., Lambert, M.P., Fernandez, S.J., Velasco, P.T., Lacor, P.N., Bigio, E.H., Jerecic, J., Acton, P.J., Shughrue, P.J., Chen-Dodson, E., Kinney, G.G., Klein, W.L., 2008. Alzheimer's disease-type neuronal tau hyperphosphorylation induced by A beta oligomers. Neurobiol. Aging 29, 1334–1347.

Di Carlo, M., Giacomazza, D., San Biagio, P.L., 2012. Alzheimer's disease: biological aspects, therapeutic perspectives and diagnostic tools. J. Phys. Condens. Matter 24, 244102.

Emilsson, L., Saetre, P., Balciuniene, J., Castensson, A., Cairns, N., Jazin, E.E., 2002. Increased monoamine oxidase messenger RNA expression levels in frontal cortex of Alzheimer's disease patients. Neurosci. Lett. 326, 56–60.

Fändrich, M., 2012. Oligomeric intermediates in amyloid formation: structure determination and mechanisms of toxicity. J. Mol. Biol. 421, 427–440.

Freitas, A.A., de Magalhães, J.P., 2011. A review and appraisal of the DNA damage theory of ageing. Mutat. Res. 728, 12–22.

Hermida-Ameijeiras, A., Méndez-Alvarez, E., Sánchez-Iglesias, S., Sanmartín-Suárez, C., Soto-Otero, R., 2004. Autoxidation and MAO-mediated metabolism of dopamine as a potential cause of oxidative stress: role of ferrous and ferric ions. Neurochem. Int. 45, 103–116.

Holtzman, D.M., 2008. Alzheimer's disease: moving towards a vaccine. Nature 454, 418–420.

Huang, X., Cuajungco, M.P., Atwood, C.S., Hartshorn, M.A., Tyndall, J.D., Hanson, G.R., Stokes, K.C., Leopold, M., Multhaup, G., Goldstein, L.E., Scarpa, R.C., Saunders, A.J., Lim, J., Moir, R.D., Glabe, C., Bowden, E.F., Masters, C.L., Fairlie, D.P., Tanzi, R.E., Bush, A.I., 1999. Cu(II) potentiation of Alzheimer abeta neurotoxicity. Correlation with cell-free hydrogen peroxide production and metal reduction. J. Biol. Chem. 274, 37111–37116.

Irie, K., Murakami, K., Masuda, Y., Morimoto, A., Ohigashi, H., Hara, H., Ohashi, R., Takegoshi, K., Fukuda, H., Nagao, M., Shimizu, T., Shirasawa, T., 2007. The toxic conformation of the 42-residue amyloid beta peptide and its relevance to oxidative stress in Alzheimer's disease. Mini Rev. Med. Chem. 7, 1001–1008.

Kent, C., Sugaya, K., Bryan, D., Personett, D., McKinney, M., 1999. Expression of superoxide dismutase messenger RNA in adult rat brain cholinergic neurons. J. Mol. Neurosci. 12, 1–10.

Leão, R.N., Colom, L.V., Borgius, L., Kiehn, O., Fisahn, A., 2012. Medial septal dysfunction by Aβ-induced KCNQ channel-block in glutamatergic neurons. Neurobiol. Aging 33, 2046–2061.

Lecanu, L., Greeson, J., Papadopoulos, V., 2006. Beta-amyloid and oxidative stress jointly induce neuronal death, amlyoid deposits, gliosis, and memory impairment in the rat brain. Pharmacology 76, 19–33.

Lin, H., Xu, H., Liang, F.Q., Liang, H., Gupta, P., Havey, A.N., Boulton, M.E., Godley, B.F., 2011. Mitochondrial DNA damage and repair in RPE associated with aging and age-related macular degeneration. Invest. Ophthalmol. Vis. Sci. 52, 3521–3529.

Marlatt, M., Lee, H.G., Perry, G., Smith, M.A., Zhu, X., 2004. Sources and mechanisms of cytoplasmic oxidative damage in Alzheimer's disease. Acta Neurobiol. Exp. (Wars.) 64, 81–87.

Murray, I.V., Liu, L., Komatsu, H., Uryu, K., Xiao, G., Lawson, J.A., Axelsen, P.H., 2007. Membrane-mediated amyloidogenesis and the promotion of oxidative lipid damage by amyloid beta proteins. J. Biol. Chem. 282, 9335–9345.

Noebels, J.A., 2011. Perfect storm: converging paths of epilepsy and Alzheimer's dementia intersect in the hippocampal formation. Epilepsia 52 (Suppl. 1), 39–46.

Paxinos, G., Watson, C., 1998. The Rat Brain in Stereotaxic Coordinates. Academic Press, New York.

Perry, G., Nunomura, A., Hirai, K., Takeda, A., Aliev, G., Smith, M.A., 2000. Oxidative damage in Alzheimer's disease: the metabolic dimension. Int. J. Dev. Neurosci. 18, 417–421.

Pfaffl, M.W., 2006. Real Time PCR (BIOS Advanced Methods). Vol., Taylor & Francis Group, New York.

Richards, J.G., Saura, J., Luque, J.M., Cesura, A.M., Gottowik, J., Malherbe, P., Borroni, E., Gray, J., 1998. Monoamine oxidases: from brain maps to physiology and transgenics to pathophysiology. J. Neural Transm. Suppl. 52, 173–187.

Santos, R.X., Correia, S.C., Wang, X., Perry, G., Smith, M.A., Moreira, P.I., Zhu, X., 2010. Alzheimer's disease: diverse aspects of mitochondrial malfunctioning. Int. J. Clin. Exp. Pathol. 3, 570–581.

Shao, C., Xiong, S., Li, G.M., Gu, L., Mao, G., Markesbery, W.R., Lovell, M.A., 2008. Altered 8-oxoguanine glycosylase in mild cognitive impairment and late-stage Alzheimer's disease brain. Free Radic. Biol. Med. 45, 813–819.

Shibutani, S., Takeshita, M., Grollman, A.P., 1991. Insertion of specific bases during DNA synthesis past the oxidation-damaged base 8-oxodG. Nature 349, 431–434.

Stevnsner, T., Thorslund, T., de Souza-Pinto, N.C., Bohr, V.A., 2002. Mitochondrial repair of 8-oxoguanine and changes with aging. Exp. Gerontol. 37, 1189–1196.

Tchou, J., Kasai, H., Shibutani, S., Chung, M.H., Laval, J., Grollman, A.P., Nishimura, S., 1991. 8-oxoguanine (8-hydroxyguanine) DNA glycosylase and its substrate specificity. Proc. Natl. Acad. Sci. U. S. A. 88, 4690–4694.

Tong, Y., Zhou, W., Fung, V., Christensen, M.A., Qing, H., Sun, X., Song, W., 2005. Oxidative stress potentiates BACE1 gene expression and Abeta generation. J. Neural. Transm. 112, 455–469.

Verghese, P.B., Castellano, J.M., Holtzman, D.M., 2011. Apolipoprotein E in Alzheimer's disease and other neurological disorders. Lancet Neurol. 10, 241–252.

Wang, W., Esbensen, Y., Kunke, D., Suganthan, R., Rachek, L., Bjørås, M., Eide, L., 2011. Mitochondrial DNA damage level determines neural stem cell differentiation fate. J. Neurosci. 31, 9746–9751.